Compact Passive Q-Switching Pr^{3+}-Doped ZBLAN Fiber Laser With Black Phosphorus-Based Saturable Absorber

Duanduan Wu, Zhiping Cai, Yile Zhong, Jian Peng, Yongjie Cheng, Jian Weng, Zhengqian Luo, *Senior Member, IEEE*, and Huiying Xu

***Abstract*—In this paper, a compact passively Q-switched praseodymium (Pr^{3+})-doped fiber laser at the wavelength of 635 nm with black phosphorus (BP) saturable absorber (SA) was first investigated. BP nanoflakes were manufactured by the liquid-phase-exfoliation method and then embedded into polyvinyl-alcohol (PVA) film for the experimental usage and a fiber pigtail mirror (FPM, by coating dielectric film onto the fiber-end face) was applied to realize a compact Pr^{3+}-doped red fiber laser. By transferring a block of the BP-PVA thin film onto the FPM and then incorporating into the compact Pr^{3+}-doped fiber laser, the Q-switched operation at 635 nm was achieved. The pulse-repetition rate of the visible-wavelength Q-switched fiber laser can be widely tuned from 108.8 to 409.8 kHz and the shortest pulse duration of this laser is 383 ns. These results reveal that the BP is an available SA for red-light lasers.**

***Index Terms*—Black phosphorus, Q-switching, wide pulse repetition-rate, narrow pulse-duration, visible fiber laser.**

I. Introduction

TWO-dimensional (2-D) materials are of great attention for optoelectronic and photonic applications because of their special optical and electronic properties. Recent research in 2-D materials primarily focuses on graphene, topological-insulators (TIs), transition-metal-dichalcogenides (TMDs) and the new black phosphorus (BP). Each type of the 2-D materials owns its unique characteristics. Graphene possesses zero bandgap nature [1], and the topological energy gaps of TIs are narrow (e.g., TI: Bi_2Se_3, $\Delta E \sim 0.3$ eV) [2] as well as the bandgaps of TMDs are comparatively large (1.1–2.0 eV) [3]. There remains a large gap between TIs and TMDs in the range of 0.3–1 eV which is important to photonic devices. Fortunately, BP, a material with tunable direct bandgap (from 0.3 (bulk) to 2.0 eV (monolayer)) [4]–[6], has recently joined in the family of 2-D materials. The emergence of the BP nanosheets can bridge the gap between TIs and TMDs. Moreover, BP also exhibits the behavior of optical bleaching if under strong light illumination, known as saturable absorption [7], [8]. Similar to other 2-D materials, BP could also serve as a wideband saturable absorber (SA) [9]–[47]. For instance, Zhang *et al.* [9] have achieved the BP-based mode-locking operation in a solid-state laser with the central wavelength of 1064.1 nm. And Sotor *et al.* have respectively reported the 272 fs short pulses generation from a 1560.5 nm Er^{3+}-doped fiber laser [10] and the 739 fs short pulses generation from a 1910 nm Tm^{3+}-doped fiber laser by using BP SAs [11]. Qin *et al.* [12] have demonstrated a 2.8 μm passive Q-switching Er^{3+}-doped ZBLAN fiber laser with a BP SA. Moreover, noted that few-layer BPs possess $\sim$2 eV direct bandgap (corresponding to the wavelength range of $\sim$600 nm), they might be utilized as visible-wavelength Q-switchers or mode-lockers to extend the operation waveband towards the visible region. Therefore, the ultrafast nonlinear optical response of BP nanoplatelets in the visible region was concerned. The saturation intensity and normalized modulation depth were respectively measured to be 455.3 ± 55 GW/cm^2 and 27.6% at the wavelength of 400 nm, 334.6 ± 43 GW/cm^2 and 12.4% at 800 nm by Lu *et al.* [7] manifesting the excellent potential as a SA in the visible spectral range. Hanlon *et al.* [8] measured the nonlinear optical properties of BP nanosheets at the visible wavelength of 515 nm. The normalized modulation depth was measured to be $\sim$14%, indicating the strong saturable absorption response of BP in the visible spectral range.

However, one could notice that there already exits several kinds of SAs working in the visible spectral ranges [38]–[42], including transition-metal-doped crystals, semiconductor-saturable-absorber-mirrors (SESAMs), and so on. For example, Kannari *et al.* have reported the usage of Cr^{4+}: YAG [38] and Cr^{4+}-doped $Y_3Al_5O_{12}$ [39] in pulsed praseodymium (Pr^{3+})-doped YLF_4 lasers, respectively. SESAM has been utilized as a mode-locker in the Pr^{3+}-doped YLF_4 laser by Gaponenko *et al.* [40]. Even so, bulky constructions of the transition-metal-doped crystals always make the lasers complex and sensitive to the environment. And SESAMs often possess complicated fabrication, costly packages and the narrow operation waveband though they have been mature and commercial so far. In contrast, the BP SAs possess the following advantages: 1) Simple production and low cost; 2) compact size and high compatibility; 3) low saturation intensity, ultrafast recovery time, and especially wideband response ranges. Therefore, the BP SAs could be preferred.

Manuscript received March 24, 2016; revised April 02, 2016; accepted April 02, 2016. This work was supported in part by the Specialized Research Fund for the Doctoral Program of Higher Education under Grant 20120121110034 and in part by the National Natural Science Foundation of China under Grant 61275050.

D. Wu, Z. Cai, Y. Zhong, Y. Cheng, Z. Luo, and H. Xu are with the Department of Electronic Engineering, Xiamen University, Xiamen 361005, China (e-mail: wdd880309@xmu.edu.cn; zpcai@xmu.edu.cn; zyl280782111@qq.com; chengyj172420041@qq.com; zqluo@xmu.edu.cn; xuhy@xmu.edu.cn).

J. Peng and J. Weng are with the Department of Biomaterials, Xiamen University, Xiamen 361005, China (e-mail: pj13545639809@126.com; jweng@xmu.edu.cn).

Color versions of one or more of the figures in this paper are available online at http://ieeexplore.ieee.org.

Digital Object Identifier 10.1109/JSTQE.2016.2550560

To integrate into the laser cavities, the BP SAs can deposite on the glass-substrate for solid-state lasers or filmy cover on the fiber-end face and coat on micro-fiber devices for fiber lasers. Compared with solid-state lasers, fiber lasers can possess high beam quality, compact design and flexibility. To realize visible fiber lasers, low-loss visible gain fiber is a key element. Pr^{3+}-doped ZBLAN fiber has been considered as an excellent visible gain medium due to the low maximum phonon-energy below 600 cm^{-1} and the low-loss less than 0.1 dB/m [43]. Meanwhile, through pumping with a blue GaN laser diode (LD), the laser efficiency could be enhanced with down-conversion of Pr^{3+} ions [44]. However, Pr^{3+}-doped ZBLAN fiber has an inherent drawback which is very difficult to directly splice with other fibers. If a visible reflection mirror is fiber-compatible (e.g., fiber pigtail mirror (FPM) by coating dielectric-film onto the fiber-end face), the visible Pr^{3+}-doped ZBLAN laser will become a compact all-fiber construction. Therefore, the combination of the compact Pr^{3+}-doped ZBLAN fiber cavity with the BP for passive pulsed operation in the visible regions would represent a attractive approach.

In this paper, we experimentally presented a compact all-fiber passive Q-switching 635 nm Pr^{3+}-doped laser with a BP SA. The tunable pulse-repetition-rate range of the Q-switching red fiber laser is 300 kHz and the pulse duration can only be 383 ns.

II. Fabrications and Characterizations of BPs

The liquid-phase-exfoliation method was used to prepare our BP nonosheets. The procedures are as follows: 1) Producing the few-layer BP suspension through adding the purchased BP (XFNANO) into a N-2-methyl pyrrolidone (NMP) solution and sonicating for 40 h; 2) removing the bulk BP by centrifuging the few-layer BP suspension at 2000 r/min for a period of 30 min; 3) removing the free NMP through decanting the supernatant to other centrifuge tubes and centrifuging at the rotate speed of 13000 r/min for a period of 30 min. X-ray diffraction (XRD) was first used to characterize the bulk BP. From Fig. 1(a), all the labeled-peaks can be easily corresponded to the orthorhombic BP (JCPDS no. 76-1957). Compared to the bulk BP, the [0 2 0] orientation in the XRD pattern of BP nanosheets is much higher. In Fig. 1(b), Raman spectroscopy of the BP materials before and after exfoliation was also characterized. The three characteristic-peaks of 361, 438, and 465 cm^{-1} are assigned to A_g^1, B_{2g} and A_g^2 modes of bulk BP. The few-layer BP samples present no obvious change of peaks when compare to bulk BP, indicating the BP nanosheets are at least three layers [45]. Furthermore, the atomic force microscopy (AFM) was used to characterize the thickness of exfoliated BP nanosheets, as can be seen in Fig. 1(c). From Fig. 1(d), the average thickness was measured to be ~2.8 nm. Since the thickness of single-layer BP is about 0.9 nm [5], these BP nanoflakes are suggested to be ~3 layers. For our practical usage, it could be preferred that the BP nanoflakes are polymer-composite structure. Therefore, we mixed the prepared BP suspension with polyvinyl-alcohol (PVA) polymer, which is favorable to form film. And then we dried the as-prepared BP-PVA solution on a glass substrate. Subsequently, the linear-absorption spectra of BP-PVA sample in a few random points were measured. As can be seen in Fig. 1(e), the linear-absorption coefficient at the concerned 635 nm is about 34% and its fluctuation can be as low as 1.7%, indicating the good uniformity of our BP-PVA sample. One could want to know the nonlinear optical property (i.e., saturable absorption property) of the BP nanosheets at the wavelength of 635 nm. However, because of the absence of ultra-short visible laser sources, we can not measure the visible-wavelength saturable absorption by the Z-scan method or the power-dependent twin-detector method [33]. However, the normalized modulation depth of BP at 635 nm could be estimated to be between 14% of 515 nm [8] and 12.4% of 800 nm [7], which could be used as promising SAs for the visible spectral ranges.

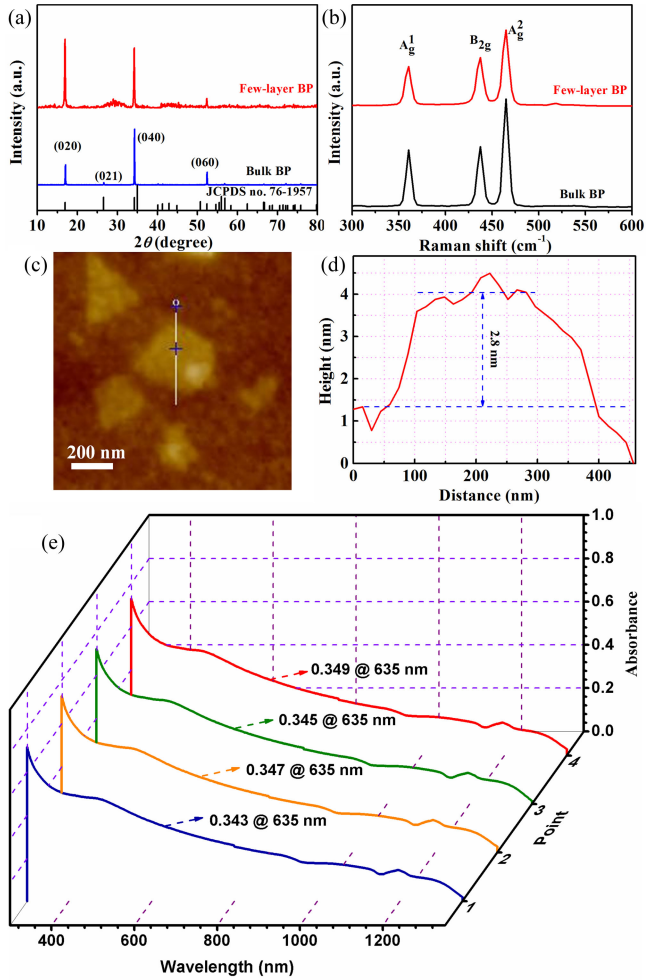

Fig. 1. (a) XRD and (b) the Raman spectra of the bulk BP and the few-layer BP. (c) AFM image and (d) the height profile diagram of the few-layer BP. (e) The linear absorbance spectra of the few-layer BP sample in four different points.

III. Experimental Structure of BPs-Based Passive Q-Switching Pr^{3+}-Doped Red Fiber Laser

Fig. 2 presents the proposed BP-based passive Q-switching 635 nm Pr^{3+}-doped ZBLAN fiber laser. The experimental setup in picture and schematic patterns is respectively given in Fig. 2(a) and (b). The pump source was a 444 nm/2 W GaN

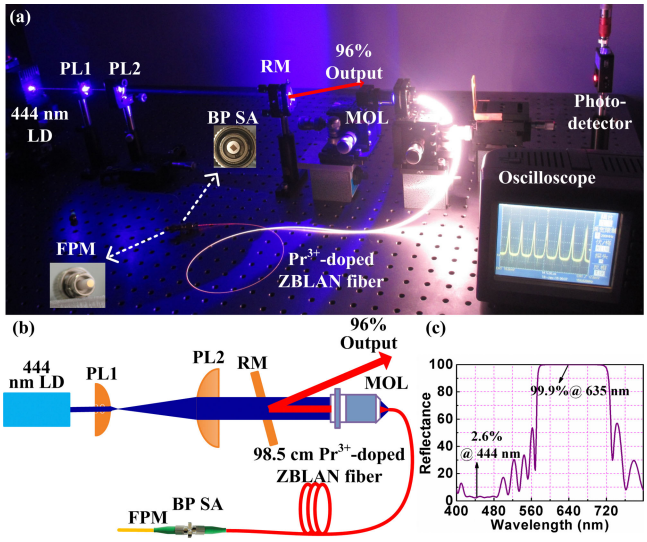

Fig. 2. (a) Picture of the proposed few-layer BP SA-based red passive Q-switching Pr^{3+}-doped fiber laser, with inserting an image of FPM and the Pr^{3+}-doped fiber face covered with a BP-PVA thin film. (b) Corresponded schematic. (c) Reflectance of the FPM.

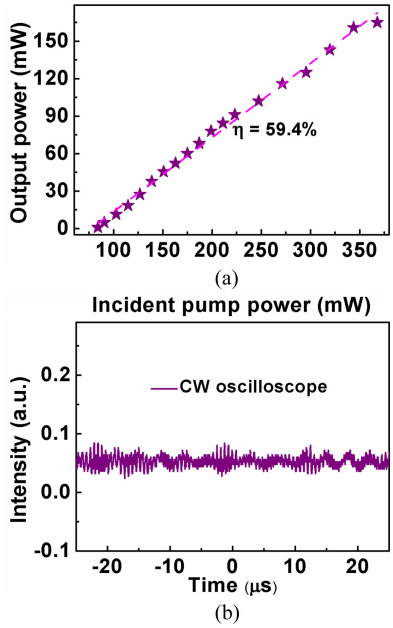

Fig. 3. (a) The output power of CW red laser versus the incident-pump-power. (b) CW oscilloscope traces [46].

LD. And the gain medium was a 98.5 cm Pr^{3+}-doped ZBLAN fiber (6/125, Pr concentration 1000 ppm). The length of the Pr^{3+}-doped ZBLAN fiber could be further optimized due to the large absorption coefficient at 444 nm. A micro-objective lens (MOL) and two plano-convex lenses constructed the pump coupling system. The coupling efficiency of the pump source into the fiber was measured to be ~17.4%. The laser resonant cavity is formed by the FPM and Fresnel reflection of Pr^{3+}-doped fiber-end face, which is a compact all-fiber configuration. Fig. 2(c) shows reflection spectrum of the FPM (by coating dielectric-film onto the fiber-end face), we can see that the reflection of the 635 nm red-light is about 99.94% and the transmittance of the 444 nm pump-light is about 97.4%, which can serve as a high efficient red fiber reflector. Inset of Fig. 2(a) gives an image of the FPM. To couple out the intra-cavity laser, a red mirror (RM, similar to the FPM, transmitting ~84% of 444 nm light and reflecting ~99% of 635 nm light) was placed before the MOL with a little angle. A piece of the few-layer BP-PVA film covered on one face of the Pr^{3+}-doped ZBLAN fiber, as shown in inset of Fig. 2(a), and then connected to the FPM to construct the fiber-compatible BP SA. The Q-switching pulse-trains, the average output-power, the output optical-spectrum, the radio-frequency (RF) spectrum, and the optical intensity distribution were respectively monitored and measured by an oscilloscope together with a photodetector, a power meter, an optical spectrum analyzer (OSA), a RF spectrum analyzer, and a laser beam analyzer (Spiricon LBA-400PC).

IV. Results and Discussions

The laser operation without a BP SA was first performed. From Fig. 3(a), the red laser appears at the incident-pump-power of about 83 mW, and the maximum output power can reach 165 mW with a slope-efficiency of 59.4% [46]. The output power could be further enhanced with higher pump sources or improving pump coupling efficiency. To confirm the continuous-wave (CW) operation, we monitored the laser output with an oscilloscope. From Fig. 3(b), no regular pulse trains can be observed. Then, a BP-PVA thin film (total loss of ~3.1 dB) was integrated into the laser. When increased the incident-pump-power to 182.7 mW, CW red laser came out. The threshold with the BP SA is higher than the one (83 mW) without the BP SA. By continually increasing the incident-pump-power to 190.6 mW, we observed the regular pulse trains on the oscilloscope screen, indicating the Q-switching operation is induced by BP SA. The Q-switching pulse trains were recorded with different pump power, just as shown in Fig. 4(a). By gradually increasing the incident-pump-power from 190.6 to 222.0 mW, the repetition rate of the Q-switching pulse can continuously range from 108.8 to 409.8 kHz. The RF signal-to-noise ratio (SNR) was used to represent the stability of the red Q-switching pulse trains. From Fig. 4(b), the SNR of the fundamental frequency peak at 409.8 kHz is measured to be ~43.7 dB, indicating our Q-switched pulse trains are stable. The wide-band RF spectrum without spectral modulation was also given in Fig. 4(c). We then recorded the fluorescence, the CW and the Q-switching spectra of different pump powers to observe the evolution of spectra. From Fig. 4(d), the BP-based Q-switching laser presents multi-wavelength oscillation which locates at about 635.4 nm and the central wavelength remains almost unchanged with different incident-pump-power. The laser mode-field distribution was also exhibited in inset of Fig. 4(d). It possesses good Gaussian-shape, confirming that our red Q-switching fiber laser is operating in the single transverse mode.

Fig. 5(a) gives the variation-tendency of the pulse repetition-rate and the pulse-duration as incident-pump-power. The repetition-rate monotonously increases when gradually increases the incident-pump-power from 190.6 to 222.0 mW,

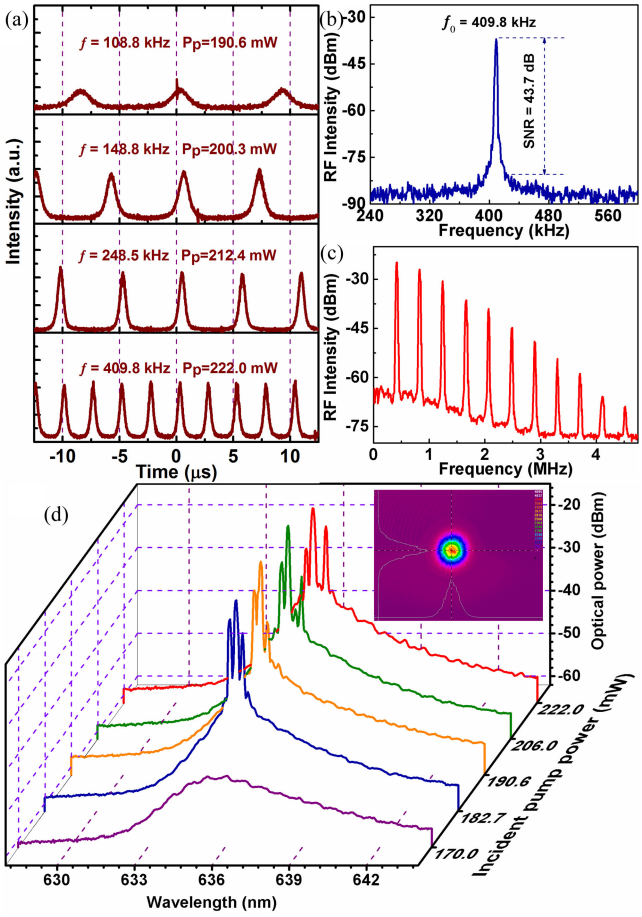

Fig. 4. (a) The oscilloscope traces of the Q-switching pulses with different pump power. (b) RF spectrum. (c) Broadband RF spectrum. (d) The evolution of spectra: the fluorescence, the CW and the Q-switching of different pump powers. Inset: laser mode-field distribution.

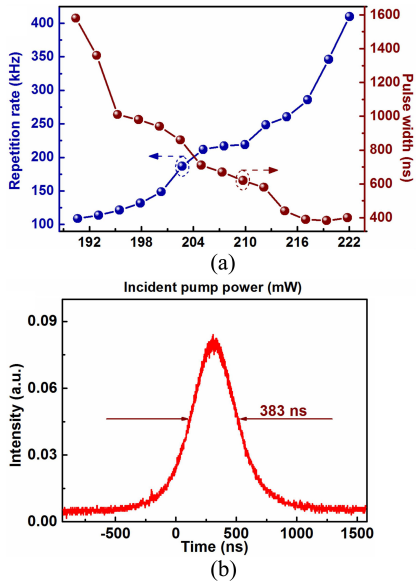

Fig. 5. (a) The pulse-repetition-rates and pulse-duration versus the incident-pump-power. (b) The narrowest pulse duration of this laser.

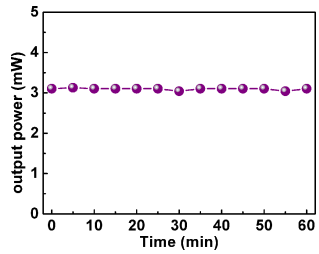

Fig. 6. The output power of the passive Q-switching red fiber laser versus the operating time at an incident-pump-power of 193 mW.

which has a wide range of 300 kHz. Meanwhile, the pulse-duration becomes shorter and shorter from 1560 to 383 ns, and then slightly increases (see Fig. 5(b)). The short cavity length makes a great contribution to the short pulse-duration. The laser output power increases linearly with a conversion efficiency of 8.1% first, and then saturated with higher incident-pump-power. The maximum output power was 4.4 mW with the incident-pump-power of 220.0 mW. Compared with CW state, the output powers and conversion efficiency under Q-switched state are much smaller which is due to the absorption or scattering of BP SA. The maximum pulse-energy was 27.6 nJ. Under higher pump intensity, the BP SA could be quickly bleached and the thermal accumulation becomes more seriously cavity, leading to the limitation of output power and pulse-energy. For these reasons, we believe higher output-power and larger pulse-energy would be enabled by optimizing the cavity parameters, such as cavity designs, BP-based SA's performance, and so on.

Since oxidation is a big issue of BP SAs, one would concern the long term stability of our red fiber laser output performance and the BP SAs. Therefore, on one hand, we measured the power stability of the Q-switching red laser. We recorded the output power every 5 min by fixing the incident-pump-power at 193 mW. FromFig. 6, the power-fluctuation is less than 2%, indicating that the passively Q-switched operation is stable. On the other hand, we reused the BP SAs after more than a month, the Q-switching operation can still reappear. In our opinion, the BPs could be somewhat isolated from the environment through mixing with PVA. However, the BP SAs could still be oxidized after a few months. In the future, much more work should still be done to solve the oxidation of the BP SAs.

At last, we compared the Q-switching output performance of the BP SA with our previous work (TMDs SAs and TIs SAs). Though with similar experimental setup, this paper still make great sense for the BP SAs as the operation waveband of BP has been extended to the visible regions. From Table I, we can see that the output-parameters of these Q-switching lasers are generally similar. Though the BP-based Q-switched laser possesses higher Q-switching threshold and longer pulse-duration, its tunable pulse-repetition-rate range is much wider. For the output power, our lasers are only a few milliwatt. However, it is just a common issue that the output powers of 2-D materials-based pulsed all-fiber lasers are always low. Nevertheless, this issue has been somewhat improved, such as in [23]. This will be the guidance of our large power visible pulsed lasers.

TABLE I
OUTPUT PARAMETERS OF RED PASSIVE Q-SWITCHING ALL-FIBER LASERS WITH DIFFERENT 2-D MATERIALS SAS

SA	Wavelength/nm	Q-switched threshold/mW	Pulse-duration /ns	Repetition-rate /kHz	Maximum Output-power/mW	Ref.
WS_2	635.1	143.6	207	232.7–512.8	8.7	[47]
MoS_2	635.5	148.4	227	240.4–438.6	7.1	
$MoSe_2$	635.4	146.8	240	357.1–555.1	6.2	
Bi_2Se_3	635.5/635.7	132.3	244	191.6–454.5	7.6	[46]
Bi_2Te_3	635.2	156.2	327	164.5–403.2	5.1	
BP	635.4	190.6	383	108.8–409.8	4.4	This paper

V. CONCLUSION

In conclusion, a BP-based 635 nm passive Q-switching Pr^{3+} -doped down-conversion all-fiber laser has been successfully proposed and investigated. FPM by coating dielectric-film was utilized for realizing all-fiber structure. The laser has a widely tunable pulse-repetition-rate range from 108.8 to 409.8 kHz and the pulse-duration can be as short as 383 ns. The results exhibit that the BP has good saturable absorption ability at the red 635 nm wavelength. In the future, BP-based 635 nm mode-locked fiber laser would be our next target. The normal dispersion and the large laser output (i.e., large-loss) of laser cavity may be the main obstacles. We will optimize the laser cavity and try to control the dispersion to realize the mode-locking operation.

REFERENCES

[1] D. C. Elias *et al.*, "Dirac cones reshaped by interaction effects in suspended graphene," *Nature Phys.*, vol. 7, no. 9, pp. 701–704, 2011.

[2] H. Zhang *et al.*, "Topological insulators in Bi_2Se_3, Bi_2Te_3, Sb_2Te_3 with a single Dirac cone on the surface," *Nature Phys.*, vol. 5, no. 6, pp. 438–442, 2009.

[3] Q. H. Wang, K. Kalantar-Zadeh, A. Kis, J. N. Coleman, and M. S. Strano, "Electronics and optoelectronics of two-dimensional transition metal dichalcogenides," *Nature Nanotechnol.*, vol. 7, no. 11, pp. 699–712, 2012.

[4] L. Li *et al.*, "Black phosphorus field-effect transistors," *Nature Nanotechnol.*, vol. 9, no. 5, pp. 372–377, 2014.

[5] H. Liu *et al.*, "Phosphorene: An unexplored 2D semiconductor with a high hole mobility," *ACS Nano*, vol. 8, no. 4, pp. 4033–4041, 2014.

[6] V. Tran, R. Soklaski, Y. F. Liang, and L. Yang, "Layer-controlled band gap and anisotropic excitons in few-layer black phosphorus," *Phys. Rev. B*, vol. 89, no. 23, 2014, Art. no. 235319.

[7] S. B. Lu *et al.*, "Broadband nonlinear optical response in multi-layer black phosphorus: an emerging infrared and mid-infrared optical material," *Opt. Exp.*, vol. 23, no. 9, pp. 11183–11194, 2015.

[8] D. Hanlon *et al.*, "Liquid exfoliation of solvent-stabilized few-layer black phosphorus for applications beyond electronics," *Nature Commun.*, vol. 6, no. 8563, 2015.

[9] B. T. Zhang *et al.*, "Exfoliated layers of black phosphorus as saturable absorber for ultrafast solid-state laser," *Opt. Lett.*, vol. 40, no. 16, pp. 3691–3694, 2015.

[10] J. Sotor, G. Sobon, W. Macherzynski, P. Paletko, and K. M. Abramski, "Black phosphorus saturable absorber for ultrashort pulse generation," *Appl. Phys. Lett.*, vol. 107, no. 5, 2015, Art. no. 051108.

[11] J. Sotor *et al.*, "Ultrafast thulium-doped fiber laser mode locked with black phosphorus," *Opt. Lett.*, vol. 40, no. 16, pp. 3885–3888, 2015.

[12] Z. P. Qin *et al.*, "Black phosphorus as saturable absorber for the Q-switched Er: ZBLAN fiber laser at 2.8 μm," *Opt. Exp.*, vol. 23, no. 19, pp. 241713–24718, 2015.

[13] T. Jiang, K. Yin, X. Zheng, H. Yu, and X. A. Cheng, (2015). "Black phosphorus as a new broadband saturable absorber for infrared passively Q-switched fiber laser," unpublished paper, 2015, [Online]. Available: http://arxiv.org/abs/1504.07341

[14] D. Li *et al.*, (2015). "Ultrafast pulse generation with black phosphorus," unpublished paper, 2015, [Online]. Available: http://arxiv.org/abs/1505.00480

[15] Z. C. Luo *et al.*, "Microfiber-based few-layer black phosphorus saturable absorber for ultra-fast fiber laser," *Opt. Exp.*, vol. 23, no. 15, pp. 20030–20039, 2015.

[16] H. R. Mu *et al.*, "Black phosporus-polymer composites for pulsed lasers," *Adv. Opt. Mater.*, vol. 3, no. 10, pp. 1447–1453, 2015.

[17] Y. Chen *et al.*, "Mechanically exfoliated black phosphorus as a new saturable absorber for both Q-switching and mode-locking laser operation," *Opt. Exp.*, vol. 23, no. 10, pp. 12823–12833, 2015.

[18] D. Li *et al.*, "Polarization and thickness dependent absorption properties of black phosphorus: new saturable absorber for ultrafast pulse generation," *Sci. Rep.*, vol. 5, 2015, Art. no. 15899.

[19] J. Ma *et al.*, "Few-layer black phosphorus based saturable absorber mirror for pulsed solid-state lasers," *Opt. Exp.*, vol. 23, no. 17, pp. 22643–22648, 2015.

[20] Y. X. Xie, L. C. Kong, Z. P. Qin, G. Q. Xie, and J. Zhang, "Black phosphorus-based saturable absorber for Q-switched Tm: YAG ceramic laser," *Opt. Eng.*, vol. 55, no. 8, 2016, Art. no. 081307.

[21] Q. L. Bao *et al.*, "Atomic-layer graphene as a saturable absorber for ultrafast pulsed lasers," *Adv. Funct. Mater.*, vol. 19, no. 19, pp. 3077–3083, 2009.

[22] Z. Q. Luo *et al.*, "Graphene-based passively Q-switched dual-wavelength erbium-doped fiber laser," *Opt. Lett.*, vol. 35, no. 21, pp. 3709–3711, 2010.

[23] D. D. Wu *et al.*, "Passive synchronization of 1.06 and 1.53 μm Q-switched fiber laser using a common graphene Q-switcher," *IEEE Photon. Technol. Lett.*, vol. 26, no. 14, pp. 1474–1477, Jul. 2014.

[24] I. H. Baek *et al.*, "Efficient mode-locking of sub-70-fs Ti: sapphire laser by graphene saturable absorber," *Appl. Phys. Exp.*, vol. 5, no. 3, 2012, Art. no. 032701.

[25] G. W. Zhu, X. S. Zhu, K. Balakrishnan, R. A. Norwood, and N. Peyghambarian, "Fe^{2+} : ZnSe and graphene Q-switched singly Ho^{3+} -doped ZBLAN fiber lasers at 3 μm," *Opt. Mater. Exp.*, vol. 3, no. 9, pp. 1365–1377, 2013.

[26] G. R. Lin and Y. C. Lin, "Directly exfoliated and imprinted graphite nano-particle saturable absorber for passive mode-locking erbium-doped fiber laser," *Laser Phys. Lett.*, vol. 8, no. 12, pp. 880–886, 2011.

[27] Z. P. Sun *et al.*, "Graphene mode-locked ultrafast laser," *ACS Nano*, vol. 4, no. 2, pp. 803–810, 2010.

[28] C. J. Zhao *et al.*, "Wavelength-tunable picosecond soliton fiber laser with Topological Insulator: Bi_2Se_3 as a mode locker," *Opt. Exp.*, vol. 20, no. 25, pp. 27888–27895, 2012.

[29] H. D. Xia *et al.*, "Ultrafast erbium-doped fiber laser mode-locked by a CVD-grown molybdenum disulfide (MoS_2) saturable absorber," *Opt. Exp.*, vol. 22, no. 14, pp. 17341–17348, 2014.

[30] M. Zhang *et al.*, "Tm-doped fiber laser mode-locked by graphene-polymer composite," *Opt. Exp.*, vol. 20, no. 22, pp. 25077–25084, 2012.

[31] J. Ma *et al.*, "Graphene mode-locked femtosecond laser at 2 μm wavelength," *Opt. Lett.*, vol. 37, no. 11, pp. 2085–2087, 2012.

[32] J. Sotor, G. Sobon, and K. M. Abramski, "Sub-130 fs mode-locked Er-doped fiber laser based on topological insulator," *Opt. Exp.*, vol. 22, no. 11, pp. 13244–13249, 2014.

[33] Z. C. Luo *et al.*, "2 GHz passively harmonic mode-locked fiber laser by a microfiber-based topological insulator saturable absorber," *Opt. Lett.*, vol. 38, no. 24, pp. 5212–5215, 2013.

[34] H. Ahmad, A. Z. Zulkifli, K. Thambiratnam, and S. W. Harun, "2.0-μm Q-Switched thulium-doped fiber laser with graphene oxide saturable absorber," *IEEE Photon. J.*, vol. 5, no. 4, 2013, Art. no. 1501108.
[35] M. W. Jung *et al.*, "A femtosecond pulse fiber laser at 1935 nm using a bulk-structured Bi_2Te_3 topological insulator," *Opt. Exp.*, vol. 22, no. 7, pp. 7865–7874, Aug. 2014.
[36] H. Zhang *et al.*, "Molybdenum disulfide (MoS_2) as a broadband saturable absorber for ultra-fast photonics," *Opt. Exp.*, vol. 22, no. 6, pp. 7249–7260, 2014.
[37] Z. Q. Luo *et al.*, "1.06 μm Q-switched ytterbium-doped fiber laser using few-layer topological insulator Bi_2Se_3 as a saturable absorber," *Opt. Exp.*, vol. 21, no. 24, pp. 29516–29522, 2013.
[38] H. Tanaka, R. Kariyama, K. Iijima, K. Hirosawa, and F. Kannari, "Saturation of 640-nm absorption in Cr^{4+}: YAG for an InGaN laser diode pumped passively Q-switched Pr^{3+}: YLF laser," *Opt. Exp.*, vol. 23, no. 15, pp. 19382–19395, 2015.
[39] R. Abe, J. Kojou, K. Masuda, and F. Kannari, "Cr^{4+}-Doped $Y_3Al_5O_{12}$ as a saturable absorber for a Q-switched and mode-locked 639-nm Pr^{3+}-doped $LiYF_4$ laser," *Appl. Phys. Exp.*, vol. 6, no. 3, 2013, Art. no. 032703.
[40] M. Gaponenko *et al.*, "SESAM mode-locked red praseodymium laser," *Opt. Lett.*, vol. 39, no. 24, pp. 6939–6941, 2014.
[41] R. Bek, H. Kahle, T. Schwarzback, M. Jetter, and P. Michler, "Mode-locked red-emitting semiconductor disk laser with sub-250 fs pulses," *Appl. Phys. Lett.*, vol. 103, no. 24, , 2013, Art. no. 242101.
[42] S. Ranta *et al.*, "Mode-locked VECSEL emitting 5 ps pulses at 675 nm," *Opt. Lett.*, vol. 38, no. 13, pp. 2289–2291, 2013.
[43] X. Zhu and N. Peyghambarian, "High-power ZBLAN glass fiber lasers: review and prospect," *Adv. Optoelectron.*, vol. 2010, 2010, Art. no. 501956.
[44] H. Okamoto, K. Kasuga, I. Hara, and Y. Kubota, "Visible-NIR tunable Pr^{3+}-doped fiber laser pumped by a GaN laser diode," *Opt. Exp.*, vol. 17, no. 22, pp. 20227–20232, 2009.
[45] J. R. Brent *et al.*, "Production of few-layer phosphorene by liquid exfoliation of black phosphorus." *Chem. Commun.*, vol. 50, no. 87, pp. 13338–13341, 2014.
[46] D. D. Wu *et al.*, "635 nm visible Pr^{3+}-doped ZBLAN fiber lasers Q-switched by topological insulators SAs," *IEEE Photon. Technol. Lett.*, vol. 27, no. 22, pp. 2379–2382, Nov. 2015.
[47] Z. C. Luo *et al.*, "Two-dimensional material-based saturable absorbers: towards compact visible-wavelength all-fiber pulsed lasers," *Nanoscale*, vol. 8, no. 2, pp. 1066–1072, 2016.

Duanduan Wu was born in Fujian, China, in 1988. She received the B.S. degree in electronics engineering from Xiamen University, Xiamen, China, in 2011, where she is currently working toward the Ph.D. degree in physics electronics. In 2015, she received the Chinese Government Overseas Study Scholarship and joined the School of Electrical and Electronic Engineering, Nanyang Technological University, Singapore.

Her research interest includes visible and infrared ultra-short pulse generation in passively Q-switched/mode-locked rare-earth-doped fiber lasers with saturable absorbers, e.g., graphene, topological insulators, black phosphorus, and so on.

Zhiping Cai was born in Fujian Province, China, in 1965. He received the Ph.D. degree from the University of Nice, Nice, France, in 1989.

He was a Senior Visiting Scholar from 1994 to 1996 and a Guest Professor from 2000 to 2001 with ENSSAT, Lannion, France. He also visited the University of Cambridge for one month in September 2013, and the Ecole Normale Suprieure for three months, in 2012. Since 1998, he has been a Full Professor with the Department of Electronic Engineering, Xiamen University, Xiamen, China. His research interests include laser physics, optoelectronics, meso-optics, and their applications. He is the author of more than 100 publications in refereed journals and conference proceedings.

Yile Zhong was born in Guangdong, China, in 1991. He received the B.S. degree in optical information science and technology from Xiamen University, Xiamen, China in 2013, where he is currently working toward the Master's degree in optical engineering.

His research interests include pulsed fiber lasers using passive saturable absorbers, e.g., graphene, topological insulator, etc.

Jian Peng was born in Hubei, China, in 1990. He received the B.S. degree in bioengineering from Yangtze University, Jingzhou, China, in 2011. He is currently working toward the Ph.D. degree in polymer chemistry and physics at Xiamen University, Xiamen, China.

His research interests include preparation and functionalization of two-dimensional materials and its application in biosensors.

Yongjie Cheng was born in Fujian, in 1987. He received the M.S. degree in optical from the Changchun University of Science and Technology, Changchun, China. He is currently working toward the Ph.D. degree in electrical science and technology at Xiamen University, Xiamen, China.

His research interests include pulsed lasers using passive saturable absorbers in DPSSL, e.g., topological insulators, transition metal dichalcogenide, and so on.

Jian Weng was born in Hubei, China, in 1974. He received the B.S. degree in material science from the Wuhan University of Technology, Wuhan, China, in 1995, the M.S. degree in material engineering from Hunan University, Changsha, China, in 1998, and the Ph.D. degree in material science from Zhejiang University, Hangzhou, China, in 2001.

During 2001–2003, he worked as a JSPS Postdoc in the Japan Science and Technology Agency. After about one year, he worked as an Associate Professor with Department of Materials, National University of Singapore. Since 2010, he has been a Full Professor of biomaterial science at Xiamen University. His research interests involve nanomaterial based biosensors, functional carbon-based nanomaterials and their applications, fabrication and applications of nobel-metal nanoparticles. He is the author and coauthor of more than 100 scientific publications and conference papers in the area of material science and engineering. He received the New Century Excellent Talents in University from the Ministry of Education of China.

Zhengqian Luo was born in Hubei, China, in 1982. He received the B.S. degree in applied physics from the Harbin Institute of Technology, China, in 2004, and the Ph.D. degree in communication engineering from Xiamen University, China, in December 2009. From 2007 to 2009, he received the Chinese Government Overseas Study Scholarship and joined the Network Technology Research Center, Nanyang Technological University, Singapore.

He is currently an Associate Professor with the School of Information Science and Technology, Xiamen University, China. His research interests include nonlinear fiber optics, optical fiber amplifiers and lasers, nanomaterial photonics, and optical access networks. He is an author or coauthor of more than 50 international journal and conference papers.

Huiying Xu was born in Fujian, China, in 1963. She received the B.S. degree in physics from Xiamen University, Xiamen, China, in 1985, and the D.E.A. from the University of Rennes I, Rennes, France, in 2001.

She is currently a Full Professor at the Department of Electronic Engineering, Xiamen University, Xiamen, China. Her research interests involve optical telecommunication, laser technology and its applications, and optical fiber devices.